

# The Stress Hormone Corticosterone Increases Synaptic $\alpha$ -Amino-3-hydroxy-5-methyl-4-isoxazolepropionic Acid (AMPA) Receptors via Serum- and Glucocorticoid-inducible Kinase (SGK) Regulation of the GDI-Rab4 Complex\*

Received for publication, July 29, 2009, and in revised form, December 24, 2009. Published, JBC Papers in Press, January 5, 2010, DOI 10.1074/jbc.M109.050229

Wenhua Liu, Eunice Y. Yuen, and Zhen Yan<sup>1</sup>

From the Department of Physiology and Biophysics, School of Medicine and Biomedical Sciences, State University of New York, Buffalo, New York 14214

Corticosterone, the major stress hormone, plays an important role in regulating neuronal functions of the limbic system, although the cellular targets and molecular mechanisms of corticosteroid signaling are largely unknown. Here we show that a short treatment of corticosterone significantly increases  $\alpha$ -amino-3-hydroxy-5-methyl-4-isoxazolepropionic acid receptor (AMPA)-mediated synaptic transmission and AMPAR membrane trafficking in pyramidal neurons of prefrontal cortex, a key region involved in cognition and emotion. This enhancing effect of corticosterone is through a mechanism dependent on Rab4, the small GTPase-controlling receptor recycling between early endosome and plasma membrane. Guanosine nucleotide dissociation inhibitor (GDI), which regulates the cycle of Rab proteins between membrane and cytosol, forms an increased complex with Rab4 after corticosterone treatment. Corticosterone also triggers an increased GDI phosphorylation at Ser-213 by the serum- and glucocorticoid-inducible kinase (SGK). Moreover, AMPAR synaptic currents and surface expression and their regulation by corticosterone are altered by mutating Ser-213 on GDI. These results suggest that corticosterone, via SGK phosphorylation of GDI at Ser-213, increases the formation of GDI-Rab4 complex, facilitating the functional cycle of Rab4 and Rab4-mediated recycling of AMPARs to the synaptic membrane. It provides a potential mechanism underlying the role of corticosteroid stress hormone in up-regulating excitatory synaptic efficacy in cortical neurons.

Adrenal corticosterone, the major stress hormone, has a potent impact on the function of several key limbic regions including hippocampus, prefrontal cortex (PFC)<sup>2</sup>, and amygdala (1–3). Emerging evidence suggests that corticosterone

influences the neurophysiology of limbic cells by modifying synaptic transmission and ion channels (4). For example, it has been found that corticosterone enhances AMPAR-mediated miniature excitatory postsynaptic current (mEPSC) amplitude and surface expression of GluR1 and GluR2 subunits in hippocampal neurons (5, 6); increases the surface mobility and synaptic content of AMPAR GluR2 subunits (7); and enhances L-type calcium currents in CA1 pyramidal neurons (8). The molecular mechanisms underlying these regulatory effects of corticosteroid signaling remain to be identified.

Corticosterone operates through mineralocorticoid receptors and glucocorticoid receptors, both of which belong to the family of nuclear receptors that bind to response elements in the DNA, thus modifying the activity of responsive genes (9, 10). One of the immediate early genes transcriptionally stimulated by corticosteroid stress hormones is the serum- and glucocorticoid-inducible kinase (SGK) (11), a family of serine/threonine kinases consisting of three isoforms. Studies in *Xenopus* oocytes have found that SGK can activate certain ion channels and transporters by increasing protein abundance in the plasma membrane (12). However, the cellular targets and functional significance of SGKs in the central nervous system are far from being understood.

Recently we have found that *in vivo* acute stressor induces a prolonged potentiation of AMPAR-mediated synaptic currents in PFC pyramidal neurons (13), which was mimicked by *in vitro* short term corticosterone treatment. The glucocorticoid receptor-triggered increase in AMPAR membrane trafficking seems to be responsible for the acute stress-induced plasticity in PFC (13). To determine how corticosterone/SGK regulates AMPARs, we focused on the Rab family small GTPases, which is a key coordinator of intracellular transport steps in exocytic and endocytic pathways (14).

In addition to cycling between inactive (GDP-bound) and active (GTP-bound) states, many Rab proteins also cycle between a membrane-bound and a cytosolic state (15), which is dependent on the GDP dissociation inhibitor (GDI (16)). GDI has the capacity to extract the inactive GDP-bound Rab from membranes and functions as a cytosolic chaperone of Rab (17). The formation of GDI-Rab complex can be stimulated by phosphorylation of GDI (18, 19), leading to accelerated exocytosis or endocytosis. In this study, we examined whether corticosterone

\* This work was supported, in whole or in part, by National Institutes of Health Grant MH 084233 (to Z. Y.).

<sup>1</sup> To whom correspondence should be addressed: Dept. of Physiology and Biophysics, State University of New York at Buffalo, 124 Sherman Hall, Buffalo, NY 14214. E-mail: zhenyan@buffalo.edu.

<sup>2</sup> The abbreviations used are: PFC, prefrontal cortex; AMPA,  $\alpha$ -amino-3-hydroxy-5-methyl-4-isoxazolepropionic acid; AMPAR, AMPA receptor; GDI, guanosine nucleotide dissociation inhibitor; SGK, serum- and glucocorticoid-inducible kinase; mEPSC, miniature excitatory postsynaptic current; HA, hemagglutinin; GST, glutathione S-transferase; DMEM, Dulbecco's modified Eagle's medium; GFP, green fluorescent protein; ANOVA, analysis of variance; CORT, corticosterone; DIV, days *in vitro*; WT, wild type; DN, dominant-negative; CA, constitutively active.

## Corticosterone Increases AMPARs via GDI-Rab4 Complex

could increase the Rab-mediated AMPAR membrane traffic via SGK-induced phosphorylation of GDI.

### MATERIALS AND METHODS

**DNA Constructs**—Rat GDI-1 and Rab4 open reading frame were cloned from rat brain cDNA by PCR, and HA or FLAG tag was added to the N-terminal of GDI in-frame. For expression in HEK293 cell or cultured neurons, GDI and Rab4 were subcloned to pcDNA3.1 vector (Invitrogen) from T/A vector. Generation of GDI mutants (S45A, S121A, S213A, and S213D) and Rab4 mutants (S27N and Q72L) was carried out with the QuikChange site-directed mutagenesis kit (Stratagene). All constructs were verified by DNA sequencing.

**Primary Neuronal Culture**—Rat PFC cultures were prepared as described previously (20, 21). In brief, frontal cortex was dissected from embryonic day 18 rat embryos, and cells were dissociated using trypsin and trituration through a Pasteur pipette. Neurons were plated on coverslips coated with poly-L-lysine in Dulbecco's modified Eagle's medium with 10% fetal calf serum at a density of  $1 \times 10^5$  cells/cm<sup>2</sup>. When neurons attached to the coverslip within 24 h, the medium was changed to Neurobasal medium with B27 supplement (Invitrogen). Cytosine arabinoside (ARAC, 5  $\mu$ M) was added at DIV 3 to stop glial proliferation. Culture neurons (DIV 18–25) were transfected with various plasmids using Lipofectamine 2000 (Invitrogen).

**Synaptic Current Recording in Neuronal Cultures**—Cultured PFC neurons (DIV 20–27) were used for recording AMPAR-mediated mEPSC as described previously (21). The external solution contained (mM): 127 NaCl, 5 KCl, 2 MgCl<sub>2</sub>, 2 CaCl<sub>2</sub>, 12 glucose, 10 HEPES, 0.001 tetrodotoxin, pH 7.3–7.4, 300–305 mosM. The *N*-methyl-D-aspartic acid (NMDA) receptor antagonist D-aminophosphonovalerate (APV, 20  $\mu$ M) and  $\gamma$ -aminobutyric acid, type A (GABA<sub>A</sub>) receptor antagonist bicuculline (10  $\mu$ M) were added to the external solution. The internal solution consisted of (in mM): 130 cesium methanesulfonate, 10 CsCl, 4 NaCl, 10 HEPES, 1 MgCl<sub>2</sub>, 5 EGTA, 2.2 QX-314, 12 phosphocreatine, 5 MgATP, 0.5 Na<sub>2</sub>GTP, 0.1 leupeptin, pH 7.2–7.3, 265–270 mosM. The membrane potential was held at  $-70$  mV during recording. The Mini Analysis program (Synapse) was used to analyze the frequency, amplitude, and decay time (the amount of time decaying from 90% to 10% of the peak) of spontaneous synaptic events over a 30-s period.

**Immunostaining in Neuronal Cultures**—Surface AMPA receptors were measured as described previously (21, 22). In brief, 2–3 days after transfection, PFC cultures were fixed in 4% paraformaldehyde (20 min, room temperature) but not permeabilized. Following the incubation with 3% bovine serum albumin (1 h) to block nonspecific staining, neurons were incubated with anti-NT-GluR1 (1:500, Upstate Biotech/Millipore) overnight at 4 °C. After three washes, neurons were incubated with Alexa Fluor 594 (red)-conjugated secondary antibody (Molecular Probes) for 2 h at room temperature. After washing in phosphate-buffered saline three times, the coverslips were mounted on slides with VECTASHIELD mounting medium.

Fluorescent images were captured with a  $\times 100$  objective and a cooled CCD camera mounted on a Nikon microscope using identical parameters and quantified with the ImageJ software.

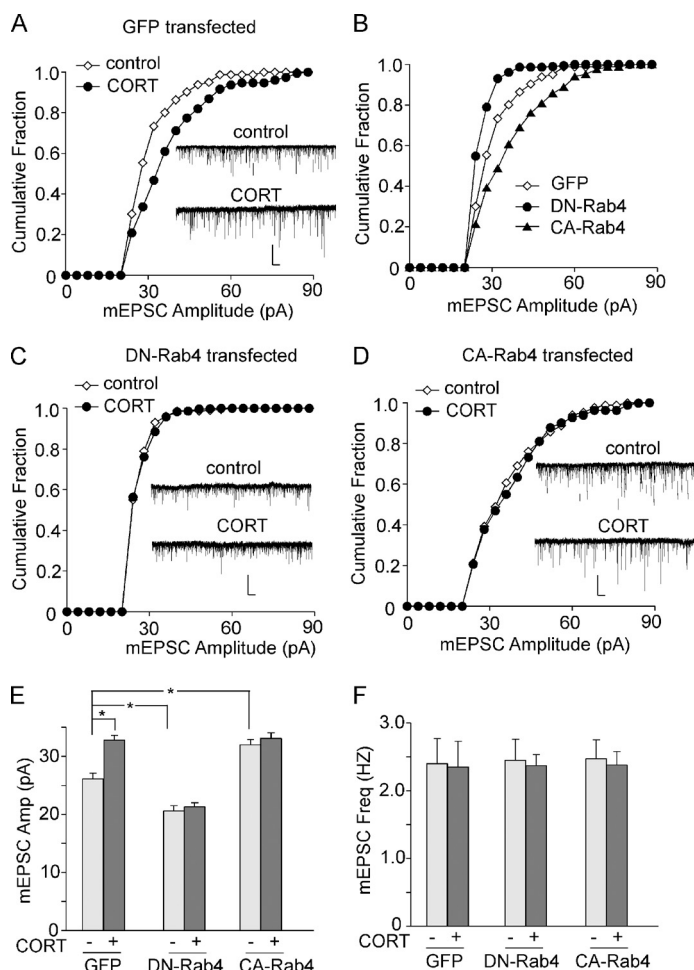


**FIGURE 1. Rab4 is involved in corticosterone regulation of synaptic AMPAR currents.** *A*, cumulative plots of the distribution of mEPSC amplitudes in untreated (control) or corticosterone (100 nM, 30 min)-treated cortical neurons transfected with GFP. *B*, cumulative plots of the distribution of mEPSC amplitudes in cultured neurons transfected with GFP alone, GFP plus dominant-negative Rab4 (DN-Rab4), or GFP plus constitutively active Rab4 (CA-Rab4). *C* and *D*, cumulative plots of the distribution of mEPSC amplitudes in untreated (control) or corticosterone-treated neurons transfected with DN-Rab4 (*C*) or CA-Rab4 (*D*). *Insets* (*A*, *C*, and *D*) show representative mEPSC traces. *Scale bars*, 30 pA, 1 s. *E* and *F*, bar graphs (mean  $\pm$  S.E.) showing the mEPSC amplitude (*mEPSC Amp*) (*E*) and mEPSC frequency (*mEPSC Freq*) (*F*) in control versus corticosterone-treated neurons transfected with different constructs.  $^*p < 0.01$ , ANOVA.

To define dendritic clusters, a single threshold was chosen manually so that clusters corresponded to puncta of 2–3-fold greater intensity than the diffuse fluorescence on the dendritic shaft. On each coverslip, the cluster density, size, and fluorescence intensity of 4–6 GFP-positive neurons (2–3 dendritic segments of  $\sim 50$   $\mu$ m/neuron) were compared. Quantitative analyses were conducted blindly.

**Co-immunoprecipitation**—HEK293 cells transfected with various FLAG-tagged GDI constructs were collected and homogenized in cold Nonidet P-40 lysis buffer (0.5% Nonidet P-40, 10% glycerol, 50 mM Tris, pH 7.6, 150 mM NaCl, 30 mM sodium pyrophosphate, 50 mM NaF, 0.1 mM EDTA, and 0.1 mM Na<sub>3</sub>VO<sub>4</sub>, 10 nM calyculin, 1 mM phenylmethylsulfonyl fluoride, 10  $\mu$ g/ml leupeptin, and protease inhibitor tablet). Lysates were ultracentrifuged (100,000  $\times g$ ) at 4 °C for 60 min. Supernatant fractions were incubated with anti-FLAG (1:1000, Sigma) for

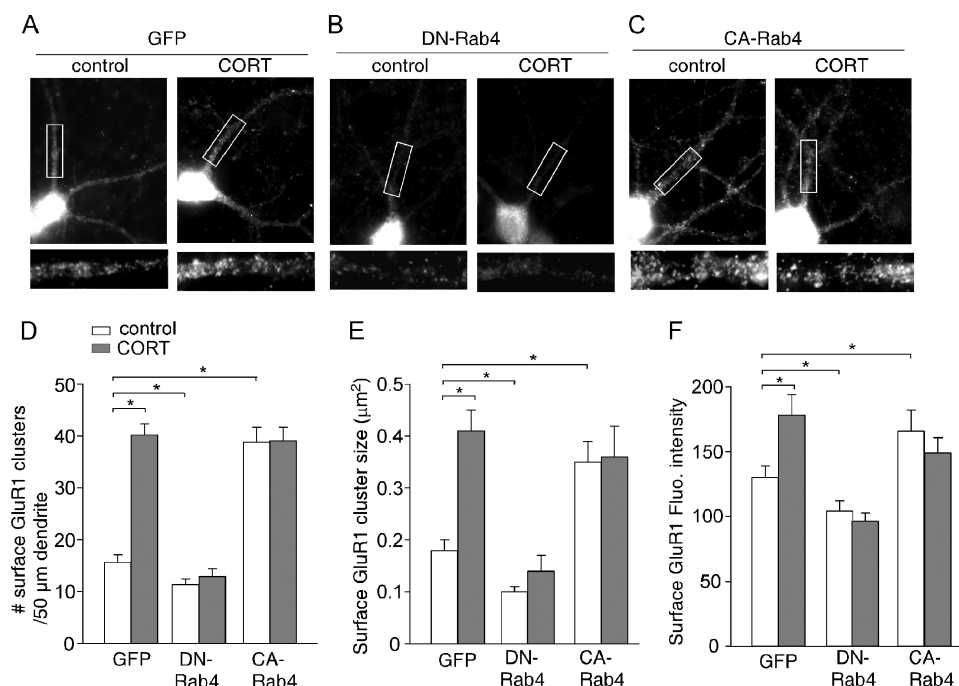


**FIGURE 2. Rab4 is involved in corticosterone regulation of AMPAR surface expression.** A–C, immunocytochemical images of surface GluR1 staining in untreated (control) or corticosterone (100 nM, 30 min)-treated cortical neurons cultures (DIV 20) transfected with GFP alone (A), GFP plus DN-Rab4 (B), or GFP plus CA-Rab4 (C). Enlarged versions of the boxed regions of dendrites are shown beneath each of the images. D–F, cumulative data (mean ± S.E.) showing the cluster density (D), cluster size (E), and fluorescence intensity (Fluo. intensity) (F) of surface GluR1 in control versus corticosterone-treated neurons transfected with different constructs. \*,  $p < 0.01$ , ANOVA.

4 h at 4 °C followed by incubation with 50 μl of protein A/G plus agarose (Santa Cruz Biotechnology) for 2 h at 4 °C. Immunoprecipitates were washed three times with lysis buffer and then boiled in 2× SDS loading buffer for 5 min and separated on 12% SDS-polyacrylamide gels. Western blotting experiments were performed with anti-Rab4 (1:1000, Santa Cruz Biotechnology).

**Expression and Purification of GST Fusion Proteins**—Wild-type GDI and its mutants S45A, S121A, and S213A were subcloned to pGEX-4T1 vector from T/A vector and transformed to BL21 *Escherichia coli* (Stratagene). Expression of GST fusion proteins was induced by treatment with 1 mM isopropyl β-D-1-thiogalactopyranoside for 3.5 h at 25 °C. Cells were collected and lysed in BugBuster protein extraction reagent (Novagen). The resulting lysate was centrifuged, and GST fusion proteins were purified with GSTrap™ HP columns (GE Healthcare).

**Phosphorylation Analysis**—HEK293 cells were grown in 6-cm dishes in 10% fetal bovine serum DMEM medium. When cells were 90% confluent, the medium was changed to 0.5% fetal bovine serum DMEM to limit serum-induced up-regulation of SGK. For *in vivo* phosphorylation analysis, the following approach was used. HA-tagged wild-type GDI or its mutants were transfected to HEK293 cells using the calcium phosphate method. One day after transfection, HEK293 cells were treated without or with 100 nM corticosterone for 30 min. Cells were then washed three times with phosphate-free DMEM medium (Invitrogen). After washing, phosphate-free DMEM medium containing 0.5% fetal bovine serum, 0.2 mCi/ml of [<sup>32</sup>P]orthophosphate (PerkinElmer Life Sciences), 100 nM calyculin, and 1 μM okadaic acid were added to cell dishes and

incubated at 37 °C for 1.5 h. After incubation, the medium was aspirated, and cells were washed twice with ice-cold phosphate-free DMEM medium. Then cells were lysed on ice with 0.5% Nonidet P-40 lysis buffer. Cell lysates were centrifuged at 16,000 × *g* at 4 °C for 20 min, and supernatants were immunoprecipitated with anti-HA (1:1000, Roche Applied Science). After washing, SDS-PAGE was carried in a 7.5% gel, and transferred membrane was subjected to autoradiography for visualizing radiolabeled proteins.

For *in vitro* phosphorylation analysis, the following approach was used. HEK293 cells were transfected with or without SGK1 small interfering RNA. One day after transfection, cells were treated without or with 100 nM corticosterone for 30 min, washed, and maintained in 0.5% fetal bovine serum DMEM for 1.5 h. Then cells were lysed in the CytoBuster protein extraction reagent (Novagen) containing protease

inhibitors. Cell lysates were centrifuged at 16,000 × *g* at 4 °C for 20 min. The supernatants (40 μl, ~50 μg of total protein) were incubated with 1 μg of purified GST fusion protein of wild-type GDI or its mutants for 30 min at 30 °C in the reaction buffer (30 mM HEPES, pH 7.5, 10 mM MgCl<sub>2</sub>, 30 μM ATP, 1 μCi of [<sup>γ</sup>-<sup>32</sup>P]ATP, 100 nM calyculin, 1 μM okadaic acid). SDS-PAGE was carried out, and phosphorylated GDI was visualized with autoradiography.

## RESULTS

**Corticosterone Treatment Increases Synaptic AMPAR Activity via Rab4-mediated Membrane Trafficking of AMPARs**—First, we examined whether corticosterone influences AMPAR-mediated synaptic currents in cultured PFC pyramidal neurons. Cells were exposed to a short treatment of corticosterone (100 nM, 30 min) and recorded at 1.5–4 h after treatment. mEPSC, which represents the postsynaptic response to release of individual vesicles of glutamate, was measured. As shown in Fig. 1A, corticosterone caused a significant enhancement of mEPSC amplitude, as indicated by a rightward shift in the distribution (control, 26.1 ± 1.0 pA,  $n = 21$ ; CORT, 32.8 ± 0.83 pA,  $n = 23$ ,  $p < 0.01$ , ANOVA, Fig. 1E). The frequency of mEPSC was not changed by corticosterone treatment (Fig. 1F). Corticosterone did not significantly change the mEPSC decay kinetics (control, 3.47 ± 0.18 ms,  $n = 18$ ; CORT, 3.63 ± 0.22 ms,  $n = 17$ ,  $p > 0.05$ , ANOVA).

The corticosterone-induced increase in glutamatergic transmission could be due to increased exocytosis/recycling of AMPARs. Thus, we investigated the potential involvement of Rab4, a member of the Rab family controlling early sorting and

## Corticosterone Increases AMPARs via GDI-Rab4 Complex

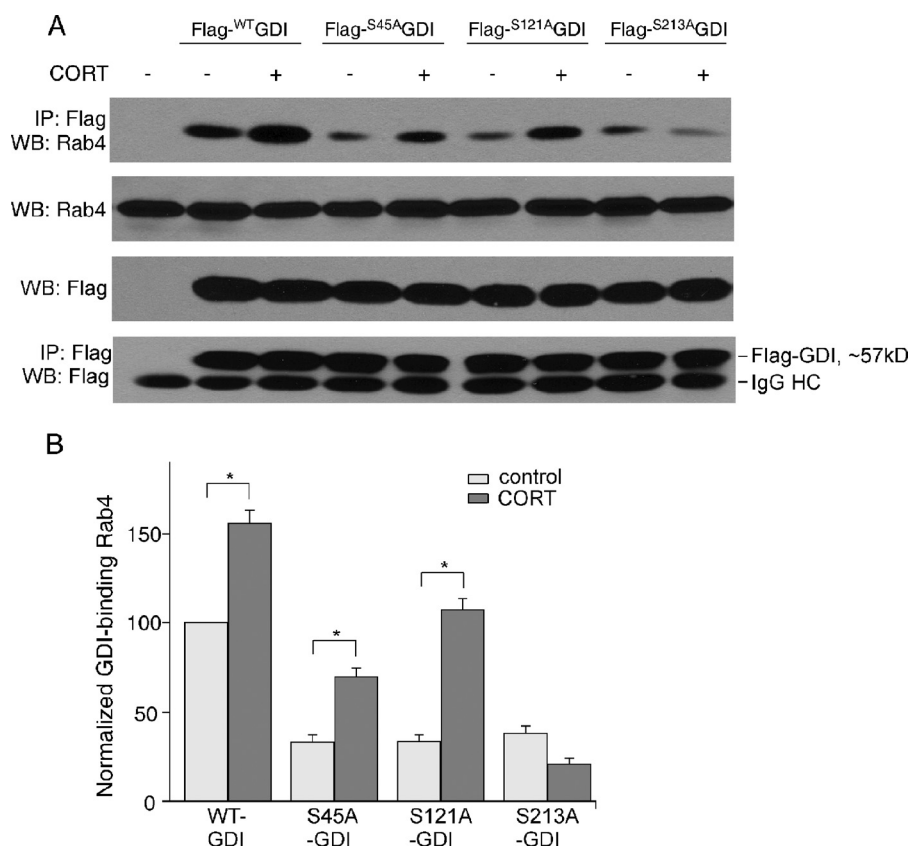


**FIGURE 3. Corticosterone treatment increases the formation of GDI-Rab4 complex, which is blocked by mutating Ser-213.** *A*, co-immunoprecipitation (IP) blots showing the level of Rab4 that binds to GDI in HEK293 cells transfected with FLAG-tagged wild-type GDI or its three mutants, S45A, S121A, S213A. After transfection, cells were treated without or with corticosterone (100 nM) for 30 min. A control for the amount of FLAG-GDI effectively immunoprecipitated is also shown. *WB*, Western blot; *HC*, heavy chain. *B*, quantification showing the normalized level of GDI-bound Rab4 in control versus corticosterone-treated HEK293 cells transfected with different GDI constructs. \*,  $p < 0.01$ , ANOVA. Data are mean  $\pm$  S.E.

recycling of proteins to the cell surface from early endosomes (14, 23, 24). Two Rab4 mutants, dominant-negative Rab4 (DN-Rab4, Rab4-S27N) or constitutively active Rab4 (CA-Rab4, Rab4-Q72L) (25), were transfected to PFC cultures. As shown in Fig. 1*B*, when compared with control neurons, transfecting DN-Rab4 caused a significant decrease of mEPSC amplitudes, whereas CA-Rab4 led to a significant enhancement of mEPSC amplitudes. The mEPSC frequency was not changed by DN-Rab4 or CA-Rab4 (Fig. 1*F*). Moreover, corticosterone failed to increase mEPSC amplitude in neurons transfected with DN-Rab4 (Fig. 1*C*, DN-Rab4,  $20.6 \pm 0.95$  pA,  $n = 13$ ; DN-Rab4+CORT,  $21.3 \pm 0.75$  pA,  $n = 15$ , Fig. 1*E*) or CA-Rab4 (Fig. 1*D*, CA-Rab4,  $32.0 \pm 0.9$  pA,  $n = 17$ ; CA-Rab4+CORT,  $33.1 \pm 0.97$  pA,  $n = 15$ , Fig. 1*E*). Taken together, these data suggest that Rab4 is involved in AMPAR recycling and that corticosterone increases synaptic AMPAR currents via a Rab4-dependent mechanism.

We further examined the impact of corticosterone on surface expression of AMPARs using immunocytochemical approaches (20–22). Surface AMPARs were measured with an antibody against the extracellular domain of GluR1 in non-permeabilized neuronal cultures. After transfection, cells were exposed to a short treatment of corticosterone (100 nM, 30 min) and stained at 2 h after treatment. As shown in Fig. 2*A*, corticosterone profoundly increased surface GluR1 cluster density

(number of clusters/50  $\mu$ m of dendrite) (control,  $15.7 \pm 1.4$ ,  $n = 20$ ; CORT,  $40.2 \pm 2.2$ ,  $n = 24$ ,  $p < 0.01$ , ANOVA, Fig. 2*D*), cluster size ( $\mu$ m<sup>2</sup>) (control,  $0.18 \pm 0.02$ ,  $n = 20$ ; CORT,  $0.41 \pm 0.04$ ,  $n = 24$ ,  $p < 0.01$ , ANOVA, Fig. 2*E*), and cluster fluorescence intensity (control,  $130.3 \pm 8.8$ ,  $n = 20$ ; CORT,  $178.0 \pm 16.0$ ,  $n = 24$ ,  $p < 0.01$ , ANOVA, Fig. 2*F*). Transfecting DN-Rab4 significantly reduced surface GluR1 cluster density, size, and intensity, whereas CA-Rab4 significantly increased them (Fig. 2, *D–F*). Furthermore, application of corticosterone failed to alter surface GluR1 clusters in neurons transfected with DN-Rab4 (Fig. 2*B*, DN-Rab4,  $11.4 \pm 1.1$  (density),  $0.1 \pm 0.01$  (size),  $104.5 \pm 7.8$  (intensity),  $n = 16$ ; DN-Rab4+CORT,  $13.0 \pm 1.4$  (density),  $0.14 \pm 0.03$  (size),  $96.3 \pm 6.6$  (intensity),  $n = 15$ ,  $p > 0.01$ , ANOVA, Fig. 2, *D* and *F*) or CA-Rab4 (Fig. 2*C*, CA-Rab4,  $38.8 \pm 2.9$  (density),  $0.35 \pm 0.04$  (size),  $165.8 \pm 16.4$  (intensity),  $n = 19$ ; CA-Rab4+CORT,  $39.1 \pm 2.6$  (density),  $0.36 \pm 0.06$  (size),  $148.8 \pm 11.9$  (intensity),  $n = 19$ ,  $p > 0.01$ , ANOVA, Fig. 2, *D–F*). These results suggest that Rab4 is involved in

AMPAR membrane trafficking and that corticosterone increases AMPAR surface expression via a Rab4-dependent mechanism.

**Corticosterone Treatment Increases GDI-Rab4 Complex—**Next, we sought to determine the mechanism underlying corticosterone enhancement of Rab4-mediated AMPAR synaptic delivery. It is known that GDI retrieves GDP-bound Rab proteins from membranes to cytosol and thus plays a key role in the recycling of Rab proteins (26, 27). Previous studies have found that GDI can be phosphorylated in cytosol, and Rab proteins predominantly interact with phosphorylated GDI (28). Thus, we tested whether corticosterone induces GDI phosphorylation, leading to increased formation of the GDI-Rab4 complex.

GDI contains 26 Ser residues, and 3 residues have been predicted to face the outer surface of the molecule based on its three-dimensional structure (19, 29), Ser-45, Ser-121, and Ser-213. Thus, we transfected HEK293 cells with FLAG-tagged wild-type GDI or non-phosphorylatable GDI mutants, S45A, S121A, and S213A. After transfection, cells were treated with corticosterone (100 nM) for 30 min. After washing for 1.5 h, cell lysates were subjected to co-immunoprecipitation assay to detect the GDI-Rab4 complex. As shown in Fig. 3, *A* and *B*, corticosterone treatment significantly increased the amount of Rab4 that binds to WT-GDI, S45A-GDI, or S121A-GDI but not S213A-GDI. The level of total Rab4 was not altered. These data

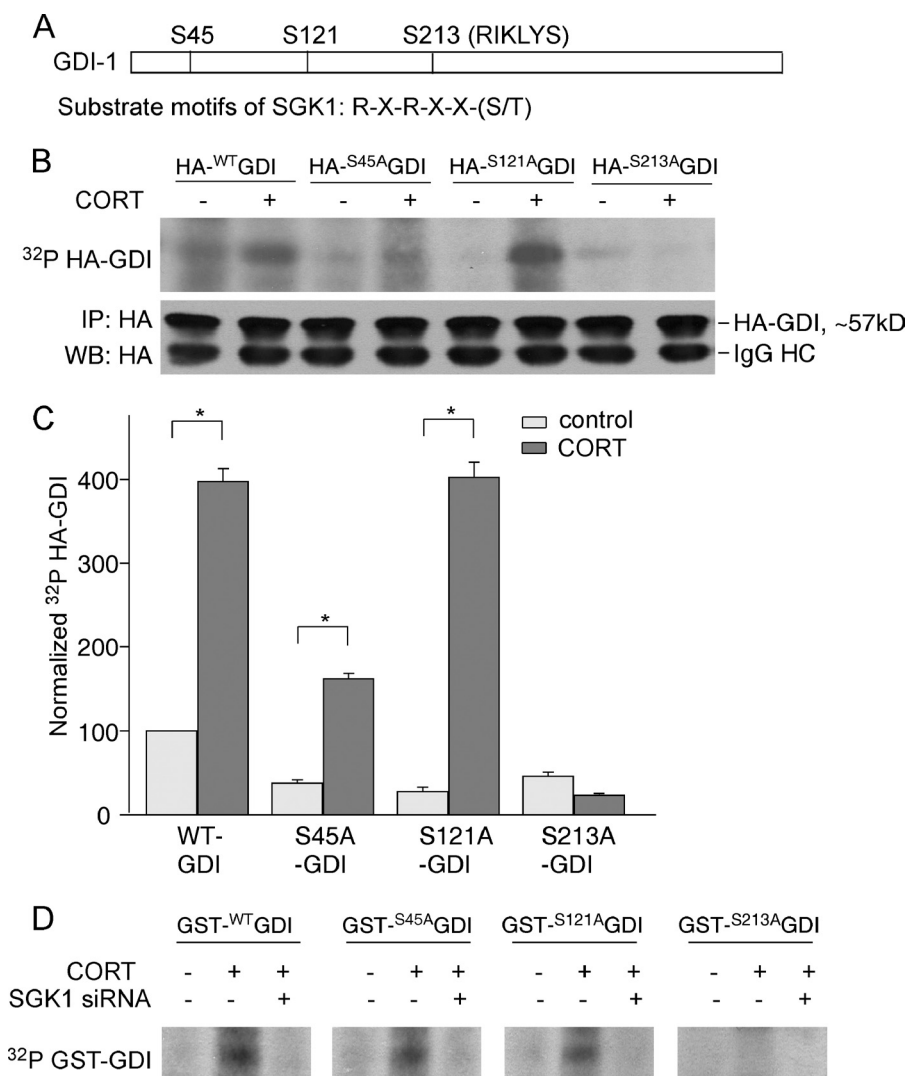


**FIGURE 4. Corticosterone treatment increases GDI phosphorylation by SGK1, which is blocked by mutating Ser-213.** *A*, diagram of rat GDI-1 protein showing the three serine sites that face the outer surface and the substrate motif of SGK1. Only Ser-213 matches the motif. *B*, representative autoradiography of GDI *in vivo* phosphorylation assay in HEK293 cells transfected with HA-tagged wild-type GDI or its three mutants. After corticosterone treatment (100 nM, 30 min), [<sup>32</sup>P]orthophosphate was incorporated into the cells. Cell lysates were immunoprecipitated (IP) with the HA antibody, and <sup>32</sup>P-labeled proteins were subjected to SDS-PAGE and visualized with autoradiography (*upper panel*). A loading control was shown in the HA blots (*lower panel*). WB, Western blot; HC, heavy chain. *C*, quantification showing the normalized radioactive intensity of <sup>32</sup>P-labeled GDI in control versus corticosterone-treated HEK293 cells transfected with different GDI constructs. \*,  $p < 0.01$ , ANOVA. Data are mean  $\pm$  S.E.D. representative autoradiography of GDI *in vitro* phosphorylation assay in HEK293 transfected without or with SGK1 small interfering RNA (siRNA). After corticosterone treatment (100 nM, 30 min), cell lysates were added to reaction tubes including 1  $\mu$ Ci of [ $\gamma$ -<sup>32</sup>P]ATP and 1  $\mu$ g of purified GST fusion protein of wild-type GDI or its three mutants. Phosphorylated GDI proteins were subjected to SDS-PAGE and visualized with autoradiography.

indicate that corticosterone increases the formation of GDI-Rab4 complex, which requires an intact Ser-213 phosphorylation site.

**Corticosterone Treatment Induces GDI Phosphorylation at Ser-213 through SGK**—The corticosteroid stress hormone exerts its function by activating mineralocorticoid receptors and glucocorticoid receptors, both of which are nuclear transcription factors that induce or repress the expression of target genes (9). Serum- and glucocorticoid-inducible kinase (SGK) is one of the downstream targets of corticosteroid signaling (11). SGK phosphorylates serine and threonine residues in the motif RXXRX(S/T), but the -3 site arginine is not quite critical for

SGK (30). To examine whether GDI is a potential substrate of SGK, we analyzed the flank sequences of Ser-45, Ser-121, and Ser-213 on GDI. We found that only the flank sequence RIKLYS of Ser-213 matched the substrate motif of SGK (Fig. 4A).

Next, we performed an *in vivo* phosphorylation assay to detect the potential GDI phosphorylation by corticosterone and the putative phosphorylation site on GDI. HA-tagged wild-type GDI and three mutants of GDI, S45A, S121A, and S213A, were transfected to HEK293 cells. After transfection, cells were treated with corticosterone (100 nM) for 30 min. After corticosterone was washed off, cells were incubated with [<sup>32</sup>P]orthophosphate-containing medium for 1.5 h. As shown in Fig. 4, *B* and *C*, <sup>32</sup>P-labeled GDI was increased remarkably by corticosterone treatment in cells transfected with WT-GDI, S45A-GDI, and S121A-GDI but not in cells transfected with S213A-GDI. These data suggest that corticosterone induces GDI phosphorylation and that Ser-213 is likely to be the phosphorylation site.

We further examined whether SGK is involved in the corticosterone-induced GDI phosphorylation. There are three SGK isoforms, SGK1, SGK2, and SGK3, and they share the same substrate motif (12, 31). The mRNAs of SGK1 and SGK3 are widely and highly expressed in all tissues, whereas SGK2 is expressed at a lower level in the brain. Furthermore, SGK1 mRNA is strongly enhanced by stimulation of glucocorticoids (31). To detect the role of SGK1 in GDI phosphorylation, we transfected SGK1 small interfering RNA in HEK293 cells to knock down its expression. After transfection and corticosterone treatment (30 min), an *in vitro* phosphorylation assay was performed by adding cell lysates to tubes containing [ $\gamma$ -<sup>32</sup>P]ATP and one of the purified recombinant GST fusion proteins, GST-WT GDI, GST-S45A GDI, GST-S121A GDI, or GST-S213A GDI. As shown in Fig. 4D, the lysates from corticosterone-treated cells induced the phosphorylation of GST-WT GDI, GST-S45A GDI, and GST-S121A GDI, but not GST-S213A GDI, and this effect was blocked in cells transfected with SGK1 small interfering RNA. These data suggest that corticosterone induces GDI phosphorylation via SGK1.

## Corticosterone Increases AMPARs via GDI-Rab4 Complex

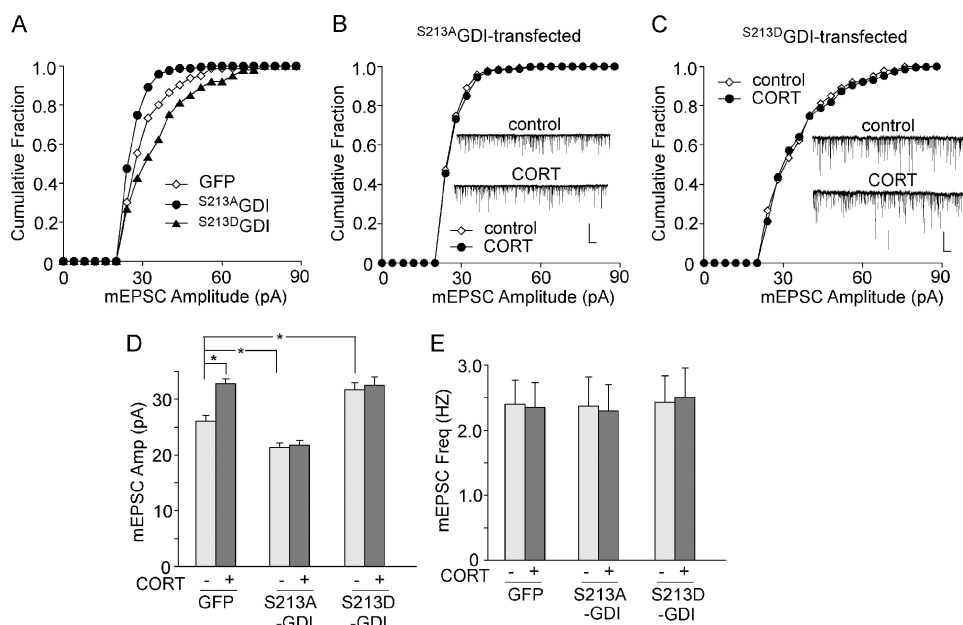


**FIGURE 5. Phosphorylation of GDI at Ser-213 is required for corticosterone regulation of synaptic AMPAR currents.** A, cumulative plots of the distribution of mEPSC amplitudes in cultured cortical neurons transfected with GFP alone, GFP plus  $S^{213A}$ GDI (non-phosphorylatable mutant), or GFP plus  $S^{213D}$ GDI (phosphomimetic mutant). B and C, cumulative plots of the distribution of mEPSC amplitudes in untreated (control) or corticosterone (100 nM, 30 min)-treated neurons transfected with  $S^{213A}$ GDI (B) or  $S^{213D}$ GDI (C). Inset, representative mEPSC traces. Scale bars, 30 pA, 1 s. D and E, bar graphs (mean  $\pm$  S.E.) showing the mEPSC amplitude (mEPSC Amp) (D) and mEPSC frequency (mEPSC Freq) (E) in control versus corticosterone-treated neurons transfected with different constructs. \*,  $p < 0.01$ , ANOVA.

*GDI Phosphorylation at Ser-213 Is Required for Corticosterone Regulation of AMPAR Synaptic Activity and Surface Expression*—Given that corticosterone increases GDI phosphorylation and the formation of GDI-Rab4 complex, we further investigated whether GDI phosphorylation could influence synaptic AMPAR activity and its regulation by corticosterone. Because Ser-213 on GDI is likely to be the SGK phosphorylation site, two constructs with mutated Ser-213 were generated. Ser-213 was mutated to alanine to represent the non-phosphorylatable form ( $S^{213A}$ ), and Ser-213 was mutated to aspartic acid to represent the phosphomimetic form ( $S^{213D}$ ). As shown in Fig. 5A, when compared with neurons transfected with GFP alone, transfecting  $S^{213A}$ GDI caused a significant decrease of mEPSC amplitude, whereas transfecting  $S^{213D}$ GDI led to a significant enhancement of mEPSC amplitude (Fig. 5D), suggesting that GDI phosphorylation at Ser-213 facilitates synaptic AMPAR activity. Furthermore, the enhancing effect of corticosterone on mEPSC amplitude was blocked by the non-phosphorylatable  $S^{213A}$ GDI (Fig. 5B,  $S^{213A}$ GDI,  $21.3 \pm 0.84$  pA,  $n = 17$ ;  $S^{213A}$ GDI+CORT,  $21.8 \pm 0.79$ ,  $n = 15$ ,  $p > 0.01$ , ANOVA, Fig. 5D) and occluded by the phosphomimetic  $S^{213D}$ GDI (Fig. 5C,  $S^{213D}$ GDI,  $31.7 \pm 1.2$  pA,  $n = 15$ ;  $S^{213D}$ GDI+CORT,  $32.5 \pm 1.5$ ,  $n = 18$ ,  $p > 0.01$ , ANOVA, Fig. 5D). The mEPSC frequency was not altered by these GDI mutants (Fig. 5E). These data suggest that corticosterone increases synaptic AMPAR currents by inducing GDI phosphorylation at Ser-213.

To confirm the role of GDI phosphorylation in corticosterone-induced AMPAR membrane delivery, we performed immunocytochemical experiments to measure AMPAR surface expression in neurons transfected with non-phosphorylat-

able or phosphomimetic GDI mutants. As shown in Fig. 6A, in GFP-transfected neurons, corticosterone treatment (100 nM, 30 min) significantly increased surface GluR1 cluster density (number of clusters/50  $\mu$ m of dendrite) (control,  $17.5 \pm 2.2$ ,  $n = 18$ ; CORT,  $33.6 \pm 3.1$ ,  $n = 17$ ,  $p < 0.01$ , ANOVA, Fig. 6D). Transfecting  $S^{213A}$ GDI caused a significant decrease of surface GluR1 cluster density and blocked the enhancing effect of corticosterone (Fig. 6B,  $S^{213A}$ GDI,  $10.3 \pm 1.8$ ,  $n = 15$ ;  $S^{213A}$ GDI+CORT,  $11.0 \pm 1.9$ ,  $n = 17$ ,  $p > 0.01$ , ANOVA, Fig. 6D). On the other hand, transfecting  $S^{213D}$ GDI significantly increased surface GluR1 cluster density and occluded the enhancing effect of corticosterone (Fig. 6C,  $S^{213D}$ GDI,  $31.0 \pm 3.5$ ,  $n = 15$ ;  $S^{213D}$ GDI+CORT,  $32.7 \pm 3.1$ ,  $n = 18$ ,  $p > 0.01$ , ANOVA, Fig. 6D). These data suggest that GDI phosphorylation at Ser-213 facilitates the

membrane trafficking of AMPARs and that corticosterone increases AMPAR surface expression via a mechanism dependent on GDI phosphorylation.

## DISCUSSION

After stress, the level of stress hormones such as corticosterone is markedly increased. Corticosterone exerts a time- and region-specific action on cellular physiology of limbic neurons (4). In this study, we have investigated the potential molecular mechanisms underlying corticosterone regulation of AMPARs in PFC neurons. The combined electrophysiological, biochemical, and immunocytochemical evidence suggests that corticosterone facilitates excitatory synaptic transmission by increasing the Rab4-mediated recycling of AMPARs to synaptic membrane via SGK1-induced phosphorylation of GDI at Ser-213.

It is well recognized that the trafficking of AMPARs plays a key role in controlling excitatory synaptic efficacy (32, 33). The internalization, recycling, or spine delivery of AMPA receptors is under the control of the Rab family of small GTPases, a key regulator for all stages of membrane traffic (34). For example, Rab5, which controls the transport from plasma membrane to early endosomes (35), is involved in clathrin-dependent AMPAR internalization (36, 37). Rab11, which mediates recycling from recycling endosomes to plasma membrane (38), controls the supply of AMPARs for long term potentiation induced by electrical stimulation (39). Rab8, which is associated with trans-Golgi network membranes, plays a role in AMPAR transport to the spine surface (40). Rab4, which controls a rapid direct recycling route from early endosomes to cell surface (24, 41), is critical for maintaining spine size (42). By using domi-

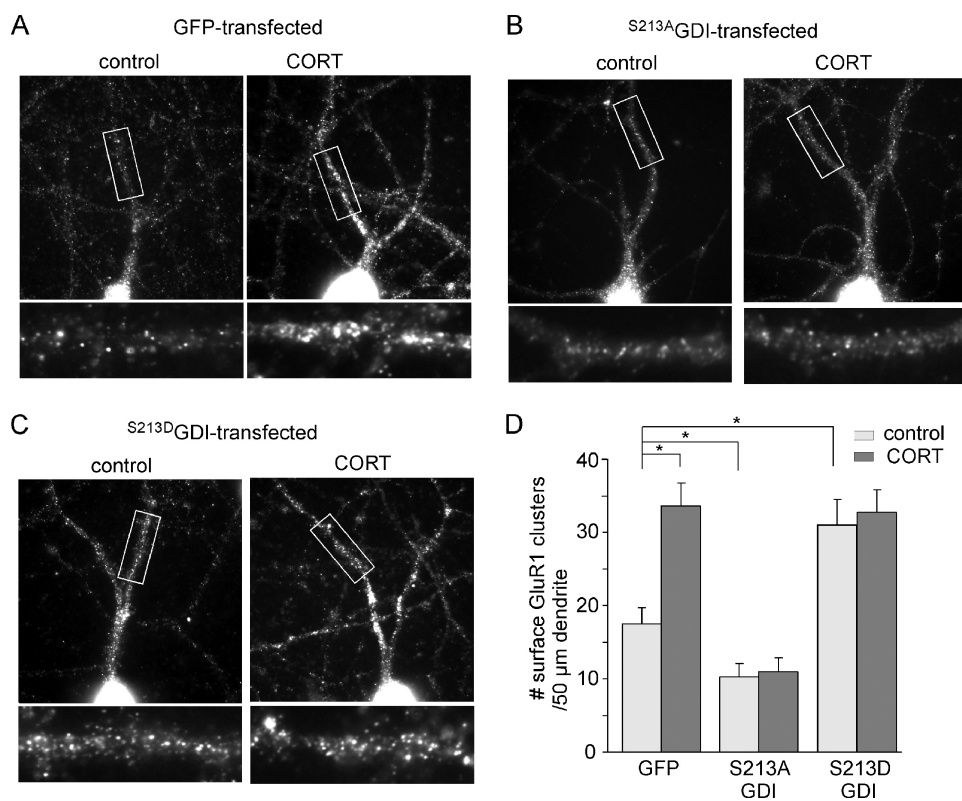


**FIGURE 6. Phosphorylation of GDI at Ser-213 is required for corticosterone regulation of AMPAR surface expression.** A–C, immunocytochemical images of surface GluR1 staining in control or corticosterone (100 nM, 30 min)-treated neurons transfected with GFP alone (A), GFP plus  $S^{213A}$ GDI (B), or GFP plus  $S^{213D}$ GDI (C). D, cumulative data (mean  $\pm$  S.E.) showing the surface GluR1 cluster density in control versus corticosterone-treated neurons transfected with different constructs. \*,  $p < 0.01$ , ANOVA.

nant-negative and constitutively active Rab4, we have demonstrated that Rab4 is not only involved in the membrane trafficking of GluR1 but also mediates the corticosterone-induced potentiation of glutamatergic transmission. Corticosterone, via activated Rab4, increases AMPAR recycling by causing its redistribution from early endosomes to the plasma membrane.

A key question is how corticosteroid signaling leads to the activation of Rab4. One possibility is through GDI, an important class of regulatory protein involved in the functional cycle and recycling of Rab GTPases (14). GDI is abundantly expressed in the brain, and the two isoforms, GDI-1 and GDI-2, share 86% identical amino acid sequence and exhibit no major functional differences (43). Biochemical assays show that GDI is able to solubilize the membrane-bound forms of Rab4 and Rab5 in a GDP/GTP-dependent manner (44). Interestingly, the phosphorylation of GDI controls its interaction with Rab proteins (28). It has been found that tyrosine phosphorylation of GDI increases the Rab4-soluble form and the GDI-Rab4 complex (18). Acute insulin treatment of cultured adipocytes, presumably by activating the downstream protein kinase B, increases cytosolic levels of Rab4 due to the formation of GDI-Rab4 complex (45). Moreover, p38 mitogen-activated protein kinase (MAPK) activates GDI and stimulates the formation of GDI-Rab5 complex by phosphorylating GDI on Ser-121, therefore facilitating the delivery of Rab5 from endosomes to the plasma membrane and accelerating endocytosis (19). Our biochemical data suggest that corticosterone activates Rab4 by

stimulating the formation of GDI-Rab4 complex via SGK1 phosphorylation of GDI.

SGKs phosphorylate serine and threonine residues lying in the motif RXXXX(S/T) (46). Because SGK has an absolute requirement for the presence of an arginine residue 5 residues N-terminal (n-5) to the site of phosphorylation (30, 31) and Ser-213 has an arginine residue at the n-5 position, Ser-213 is the most likely phosphorylation site by SGK. Our mutation experiments confirm that corticosterone/SGK-induced phosphorylation of GDI is at Ser-213.

To further demonstrate that the GDI phosphorylation at Ser-213 underlies corticosterone-induced synaptic plasticity, we have directly tested the impact of non-phosphorylatable or phosphomimetic GDI mutants on the AMPAR and its regulation by corticosterone. The non-phosphorylatable  $S^{213A}$ GDI reduces AMPAR trafficking/function and blocks the enhancing effect of corticosterone, whereas phosphomimetic  $S^{213D}$ GDI increases AMPAR

trafficking/function and occludes the enhancing effect of corticosterone. It suggests that corticosteroid signaling facilitates excitatory synaptic transmission by increasing GDI phosphorylation at Ser-213.

In summary, we have revealed a potential mechanism for corticosterone regulation of AMPARs. These stress hormone-induced changes in glutamatergic transmission could alter cognitive functions subserved by PFC (13). Understanding molecular and cellular mechanisms underlying the actions of corticosterone will provide valuable targets for designing novel therapies that modify the neuronal stress response (47).

*Acknowledgments*—We thank Xiaqing Chen and Dr. Houbo Jiang for excellent technical support.

## REFERENCES

- McEwen, B. S. (1999) *Annu. Rev. Neurosci.* **22**, 105–122
- McEwen, B. S. (2007) *Physiol. Rev.* **87**, 873–904
- de Kloet, E. R., Joëls, M., and Holsboer, F. (2005) *Nat. Rev. Neurosci.* **6**, 463–475
- Joëls, M., Krugers, H. J., Lucassen, P. J., and Karst, H. (2009) *Brain Res.* **1293**, 91–100
- Karst, H., and Joëls, M. (2005) *J. Neurophysiol.* **94**, 3479–3486
- Martin, S., Henley, J. M., Holman, D., Zhou, M., Wiegert, O., van Spronsen, M., Joëls, M., Hoogenraad, C. C., and Krugers, H. J. (2009) *PLoS One* **4**, e4714
- Groc, L., Choquet, D., and Chaouloff, F. (2008) *Nat. Neurosci.* **11**, 868–870
- Chameau, P., Qin, Y., Spijker, S., Smit, G., and Joëls, M. (2007) *J. Neuro-*

## Corticosterone Increases AMPARs via GDI-Rab4 Complex

- physiol.* **97**, 5–14
- Funder, J. W. (1997) *Annu. Rev. Med.* **48**, 231–240
  - Lu, N. Z., Wardell, S. E., Burnstein, K. L., Defranco, D., Fuller, P. J., Giguere, V., Hochberg, R. B., McKay, L., Renoir, J. M., Weigel, N. L., Wilson, E. M., McDonnell, D. P., and Cidlowski, J. A. (2006) *Pharmacol. Rev.* **58**, 782–797
  - Webster, M. K., Goya, L., Ge, Y., Maiyar, A. C., and Firestone, G. L. (1993) *Mol. Cell. Biol.* **13**, 2031–2040
  - Lang, F., Böhmer, C., Palmada, M., Seeböhm, G., Strutz-Seeböhm, N., and Vallon, V. (2006) *Physiol. Rev.* **86**, 1151–1178
  - Yuen, E. Y., Liu, W., Karatsoreos, I. N., Feng, J., McEwen, B. S., and Yan, Z. (2009) *Proc. Natl. Acad. Sci. U.S.A.* **106**, 14075–14079
  - Zerial, M., and McBride, H. (2001) *Nat. Rev. Mol. Cell Biol.* **2**, 107–117
  - Mohrmann, K., Gerez, L., Oorschot, V., Klumperman, J., and van der Sluijs, P. (2002) *J. Biol. Chem.* **277**, 32029–32035
  - Sasaki, T., Kikuchi, A., Araki, S., Hata, Y., Isomura, M., Kuroda, S., and Takai, Y. (1990) *J. Biol. Chem.* **265**, 2333–2337
  - Novick, P., and Zerial, M. (1997) *Curr. Opin. Cell Biol.* **9**, 496–504
  - Shisheva, A., Chinni, S. R., and DeMarco, C. (1999) *Biochemistry* **38**, 11711–11721
  - Cavalli, V., Vilbois, F., Corti, M., Marcote, M. J., Tamura, K., Karin, M., Arkininstall, S., and Gruenberg, J. (2001) *Mol. Cell* **7**, 421–432
  - Yuen, E. Y., Jiang, Q., Chen, P., Gu, Z., Feng, J., and Yan, Z. (2005) *J. Neurosci.* **25**, 5488–5501
  - Gu, Z., Liu, W., and Yan, Z. (2009) *J. Biol. Chem.* **284**, 10639–10649
  - Yuen, E. Y., and Yan, Z. (2009) *J. Neurosci.* **29**, 550–562
  - Van Der Sluijs, P., Hull, M., Zahraoui, A., Tavitian, A., Goud, B., and Mellman, I. (1991) *Proc. Natl. Acad. Sci. U.S.A.* **88**, 6313–6317
  - van der Sluijs, P., Hull, M., Webster, P., Måle, P., Goud, B., and Mellman, I. (1992) *Cell* **70**, 729–740
  - Odley, A., Hahn, H. S., Lynch, R. A., Marreez, Y., Osinska, H., Robbins, J., and Dorn, G. W., 2nd (2004) *Proc. Natl. Acad. Sci. U.S.A.* **101**, 7082–7087
  - Araki, S., Kikuchi, A., Hata, Y., Isomura, M., and Takai, Y. (1990) *J. Biol. Chem.* **265**, 13007–13015
  - Pfeffer, S. R., Dirac-Svejstrup, A. B., and Soldati, T. (1995) *J. Biol. Chem.* **270**, 17057–17059
  - Steele-Mortimer, O., Gruenberg, J., and Clague, M. J. (1993) *FEBS Lett.* **329**, 313–318
  - Schalk, I., Zeng, K., Wu, S. K., Stura, E. A., Matteson, J., Huang, M., Tandon, A., Wilson, I. A., and Balch, W. E. (1996) *Nature* **381**, 42–48
  - Kobayashi, T., and Cohen, P. (1999) *Biochem. J.* **339**, 319–328
  - Kobayashi, T., Deak, M., Morrice, N., and Cohen, P. (1999) *Biochem. J.* **344**, 189–197
  - Malinow, R., and Malenka, R. C. (2002) *Annu. Rev. Neurosci.* **25**, 103–126
  - Derkach, V. A., Oh, M. C., Guire, E. S., and Soderling, T. R. (2007) *Nat Rev Neurosci* **8**, 101–113
  - Pfeffer, S. R. (2001) *Trends Cell Biol.* **11**, 487–491
  - Bucci, C., Parton, R. G., Mather, I. H., Stunnenberg, H., Simons, K., Hoflack, B., and Zerial, M. (1992) *Cell* **70**, 715–728
  - Brown, T. C., Tran, I. C., Backos, D. S., and Esteban, J. A. (2005) *Neuron.* **45**, 81–94
  - Zhong, P., Liu, W., Gu, Z., and Yan, Z. (2008) *J. Physiol.* **586**, 4465–4479
  - Ullrich, O., Reinsch, S., Urbé, S., Zerial, M., and Parton, R. G. (1996) *J. Cell Biol.* **135**, 913–924
  - Park, M., Penick, E. C., Edwards, J. G., Kauer, J. A., and Ehlers, M. D. (2004) *Science.* **305**, 1972–1975
  - Gerges, N. Z., Backos, D. S., and Esteban, J. A. (2004) *J. Biol. Chem.* **279**, 43870–43878
  - Sheff, D. R., Daro, E. A., Hull, M., and Mellman, I. (1999) *J. Cell Biol.* **145**, 123–139
  - Brown, T. C., Correia, S. S., Petrok, C. N., and Esteban, J. A. (2007) *J. Neurosci.* **27**, 13311–13315
  - Yang, C., Slepnev, V. I., and Goud, B. (1994) *J. Biol. Chem.* **269**, 31891–31899
  - Shisheva, A., Südhof, T. C., and Czech, M. P. (1994) *Mol. Cell. Biol.* **14**, 3459–3468
  - Shisheva, A., and Czech, M. P. (1997) *Biochemistry.* **36**, 6564–6570
  - Lang, F., and Cohen, P. (2001) *Sci. STKE.* **2001**, re17
  - Kaufer, D., Ogle, W. O., Pincus, Z. S., Clark, K. L., Nicholas, A. C., Dinkel, K. M., Dumas, T. C., Ferguson, D., Lee, A. L., Winters, M. A., and Sapolsky, R. M. (2004) *Nat. Neurosci.* **7**, 947–953